

Measurement of hybrid content of heavy quarkonia using lattice NRQCD

Tommy Burch, Kostas Orginos*, and Doug Toussaint
Department of Physics, University of Arizona, Tucson, AZ 85721, USA
 (February 9, 2019)

Abstract

Using lowest-order lattice NRQCD to create heavy meson propagators and applying the spin-flip interaction, $c_B \frac{-g}{2m_q} \vec{\sigma} \cdot \vec{B}$, at varying intermediate time slices, we compute the off-diagonal matrix element of the Hamiltonian for the quarkonium-hybrid two-state system. Thus far, we have results for one set of quenched lattices with an interpolation in quark mass to match the $J^{PC} = 1^{--}$ bottomonium spectrum. After diagonalization of the two-state Hamiltonian, we find the ground state of bottomonium to show a $0.0035(1)c_B^2$ (with $c_B^2 \sim 1.5 - 3.1$) probability admixture of hybrid, $|Q\bar{Q}g\rangle$.

11.15Ha,12.38.G

Typeset using REVTeX

*Present address: RIKEN-BNL Research Center, Bldg 510a, Upton, NY 11973-5000

I. INTRODUCTION

In quantum chromodynamics (QCD), it has been known for some time that mesons ($q\bar{q}$) and baryons (qqq) are not the only composite states for which gauge-invariant propagators may be constructed. Multi-quark states ($qq\bar{q}\bar{q}$, $qqqq\bar{q}$, etc.) and states with gluonic excitations, or hybrids ($q\bar{q}g$, $qqqg$, etc.), can also form the necessary color singlet. It is possible for these states to have quantum numbers (J^{PC}) different from those allowed for typical hadrons. Such states are termed “exotics” and while they offer significant promise for hybrid and multi-quark state detection, they will not be the subject of our discussion here. Instead, we focus on “non-exotic” heavy hybrid mesons ($|Q\bar{Q}g\rangle$), those which have quarkonium-like quantum numbers. The true, heavy meson ground state should thus be a mixture of heavy quarkonium and hybrid:

$$|\Upsilon\rangle = A_0|Q\bar{Q}\rangle + A_1|Q\bar{Q}g\rangle + \dots \quad (1)$$

Heavy quarks within the bound state move with relatively small velocities and thus we expect the rest mass of the quarks to dominate the energy ($K \ll m_q$). Expanding in the quantity $\frac{1}{m_q}$, one finds a non-relativistic approximation to the heavy-quark Hamiltonian (NRQCD) [1]. For simplicity, we keep only the lowest-order kinetic term of the NRQCD Hamiltonian and the lowest-order spin-dependent term:

$$H = H_0 + \delta H = \frac{-\vec{D}^2}{2m_q} + c_B \frac{-g}{2m_q} \vec{\sigma} \cdot \vec{B} + \dots, \quad (2)$$

where \vec{D} is the covariant derivative. Using only the first term in this expansion, the Hamiltonian lacks a spin-flip interaction and there is no mixing between the lowest-lying hybrid and quarkonium states. For the $J^{PC} = 1^{--}$ system, the total quark spin is 1 in the S-wave state, while in the hybrid the gluonic excitation carries the angular momentum and the total quark spin is 0. Thus, our operational definition of the hybrid component of a 1^{--} meson is the component with total quark spin of 0. Inclusion of the spin-dependent term allows the mixing of these two states (see Fig. 1). Degeneracies are also lifted with the inclusion of this interaction: e.g., the $0^{-+}/1^{--}$ mass difference is due to the hyperfine spin-spin interaction and is quadratically dependent upon this term. Without the $\vec{\sigma} \cdot \vec{B}$, these states are degenerate, as are the P-wave states: $0^{++}, 1^{++}, 2^{++}$.

NRQCD has been used previously at this order, and beyond, to study heavy hybrids [2,3] and last year Drummond *et al.* [3] reported seeing no quadratic dependence of the 1^{--} magnetic hybrid mass upon the normalization of the $\vec{\sigma} \cdot \vec{B}$ term, thereby measuring no appreciable intermediate mixing with the S-wave state.

FIGURES

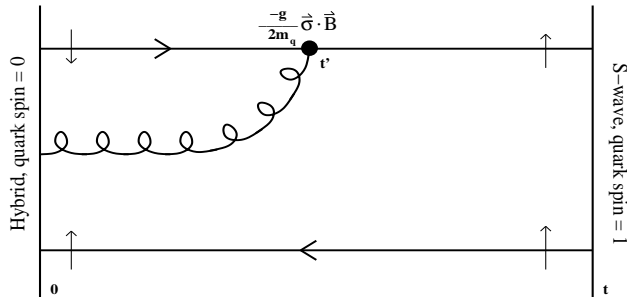


FIG. 1. Mixing of a 1^{--} magnetic hybrid with a 1^{--} S-wave via a single application of the $\vec{\sigma} \cdot \vec{B}$ interaction.

We apply a different strategy to measure the effect of the spin-dependent interaction. Rather than apply this term at every intermediate time slice in the lattice quark propagator, as is the usual practice, we restrict it to a particular intermediate time slice. Using the non-exotic hybrid source and the appropriate quarkonium sink (or vice versa), we extract the off-diagonal matrix element of the $\vec{\sigma} \cdot \vec{B}$ interaction for this two-state system, thereby determining the amount of non-exotic hybrid admixture within the true ground-state. We expect that such a result may be useful for studies of the creation and decay of heavy quarkonia via color-octet channels (see, e.g., Ref. [4]) and models of heavy-quark confinement [5].

II. THE METHOD

We construct our lattice meson propagators using the NRQCD approach. This effectively turns what would be a boundary value problem - determining the relativistic quark propagators on a periodic lattice - into an initial value problem since, in the non-relativistic limit, the quarks propagate only forward in time. Using this method, the evolution of the quark propagator in the Euclidean time direction is given by:

$$G(\vec{x}, t + a) = \left(1 - \frac{aH_0}{2n}\right)^n U_t^\dagger(x) \left(1 - \frac{aH_0}{2n}\right)^n \cdot (1 - \delta_{t',t} a \delta H) G(\vec{x}, t), \quad (3)$$

where H_0 and δH are given above and n is a parameter needed for numerical stability [6] ($n > \frac{3}{2m_q a}$; we use $n = 2$). We also use plaquette tadpole improvement of the gauge links. Note that we apply the interaction term, δH , at only a single intermediate time step, t' .

We use an incoherent sum of point sources: at the source end, we start with a given quark color and spin at all spatial points, without fixing the gauge; at the sink end, we sum over all the contributions where the quark and anti-quark are at the same spatial point. Since the lattices are not gauge-fixed, we expect the contributions from sources with the quark and anti-quark at different spatial points to average to zero. We combine the quark and anti-quark sources (propagators) with the appropriate spin matrices to construct the meson operators at the source (sink) time slices. The meson operators we use are displayed in Table III. The magnetic field is calculated using the “clover formulation” (average of field from 4 plaquettes with corners at these points):

$$\begin{aligned}
\mathcal{F}_{\mu\nu}(x) = & \frac{1}{8} [U_\mu(x)U_\nu(x + \hat{\mu})U_\mu^\dagger(x + \hat{\nu})U_\nu^\dagger(x) \\
& + U_\nu(x)U_\mu^\dagger(x + \hat{\nu} - \hat{\mu})U_\nu^\dagger(x - \hat{\mu})U_\mu(x - \hat{\mu}) \\
& + U_\mu^\dagger(x - \hat{\mu})U_\nu^\dagger(x - \hat{\nu} - \hat{\mu})U_\mu(x - \hat{\nu} - \hat{\mu})U_\nu(x - \hat{\nu}) \\
& + U_\nu^\dagger(x - \hat{\nu})U_\mu(x - \hat{\nu})U_\nu(x - \hat{\nu} + \hat{\mu})U_\mu^\dagger(x) \\
& - h.c.].
\end{aligned} \tag{4}$$

It is this form of the chromo-magnetic field (with the appropriate tadpole factor: $1/u_0^4$) that appears in the interaction term (δH). The field used to make the hybrid sources and sinks is constructed in the same fashion, with one exception: we use smeared links (sum of the simple link and all 3-staples connecting neighboring lattice sites) in place of the simple links in Eq. (4), the object being to improve the overlap with the hybrid ground state.

Since we are working on lattices with a Euclidean metric (i.e., time is imaginary), the propagators should follow decaying exponentials. The form we use to fit the meson correlators, $C(t)$, follows:

$$C(t) = A_0 e^{-m_0 t} + A_1 e^{-m_1 t}. \tag{5}$$

We include the second term to account for excited-state contributions. The propagators were averaged over a set of quenched lattices with Symanzik 1-loop improved gauge action.

To set the physical scale of our lattices, we use the S-P (spin-averaged) mass difference for bottomonium, a quantity relatively insensitive to the quark mass. We also create non-zero momentum operators for the 1^{--} S-wave meson and determine its kinetic mass from the resulting dispersion relation. An interpolation in m_q is then performed to match this kinetic mass with the experimentally determined value for the mass of the Υ . This provides us with an estimate of the bottom quark mass, m_b .

For the “mixed” propagators (different source and sink operators), we expect a propagator of the form

$$\begin{aligned}
C_{mix}(t) = & A_{0,source}^{1/2} A_{0,sink}^{1/2} \left\langle 1^{--}(H) \left| c_B \frac{-g}{2m_q} \vec{\sigma} \cdot \vec{B} \right| 1^{--}(S) \right\rangle \\
& \cdot e^{-m_{0,source} t'} e^{-m_{0,sink}(t-t')} + \dots
\end{aligned} \tag{6}$$

Knowing the amplitudes and masses of the source and sink operators from their “unmixed” propagators and fitting this propagator in the region $t > t'$, we can extract the matrix element from the amplitude of $C_{mix}(t)$ at different values of t' . At sufficiently large values of t' , we expect less excited-state contamination from the source operator and hope to find a plateau in the value of the matrix element.

For these mixed propagators, we use the tree-level value for the renormalization factor, $c_B = 1$, in the interaction term. The final result for the matrix element, however, should contain the appropriate factor for the given value of the lattice spacing. To address this, we choose a non-perturbative approach. We perform additional spectrum runs, applying the interaction term (with $c_B = 1$ and 2) at all intermediate time slices and for both the quark and anti-quark. By interpolating in the resulting values of the $0^{++}/1^{--}$ mass difference to that of experiment (or, in the present case of the $b\bar{b}$ system, potential model results), a value for c_B^2 may be found.

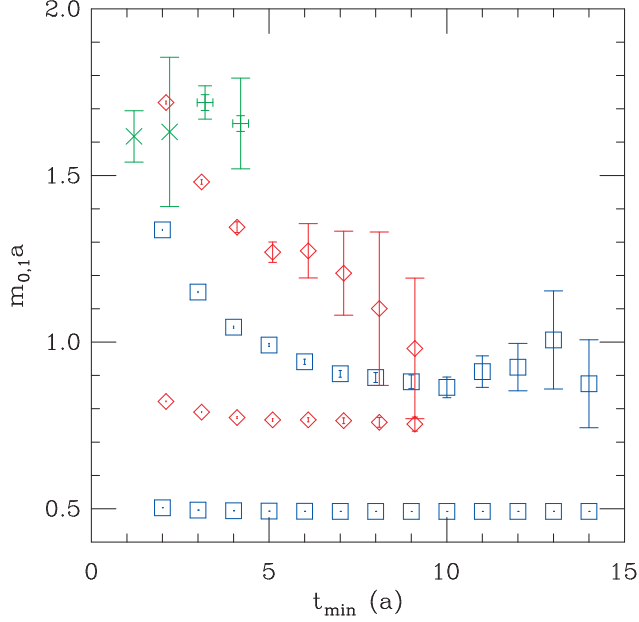


FIG. 2. Fit masses (above the zero point, E_0) vs. minimum time slice for the $1^{--}(\text{S})$ (squares), $0^{++}(\text{P})$ (diamonds), and 1^{--} hybrid (cross: two-mass fit; fancy plus: single-mass fit) with $m_q a = 2.5$. For the $1^{--}(\text{S})$ and $0^{++}(\text{P})$, both ground state and first-excited state masses are shown.

III. RESULTS

The meson correlators were averaged over 165 quenched, $20^3 \times 64$, $\beta = 8.0$ lattices with Symanzik 1-loop improved gauge action (see Ref. [7] for more details on these lattices). Shown in Fig. 2 are the fit masses for the $1^{--}(\text{S})$ and $0^{++}(\text{P})$ (ground and first-excited state), and the 1^{--} hybrid (ground state only). The results of our chosen fits to the correlators appear in Table III. Using the spin-averaged 1S-1P mass difference of 440 MeV for bottomonium, we find an inverse lattice spacing of $a^{-1} = 1604(25)$ MeV [$a = 0.123(2)$ fm]. This differs from a previous determination of the lattice spacing for this set of lattices using the quantity r_1/a from the static quark potential [7]: $a^{-1} = 1449(4)$ MeV [$a = 0.1360(3)$ fm].

Using two values of the quark mass, $m_q a = 2.5$ and 2.8, we were able to interpolate to a physical quark mass by fixing the kinetic S-wave mass to that of experiment ($M_\Upsilon = 9.46$ GeV). We find a lattice-regularized bottom quark mass of $m_b \approx 4.18$ GeV.

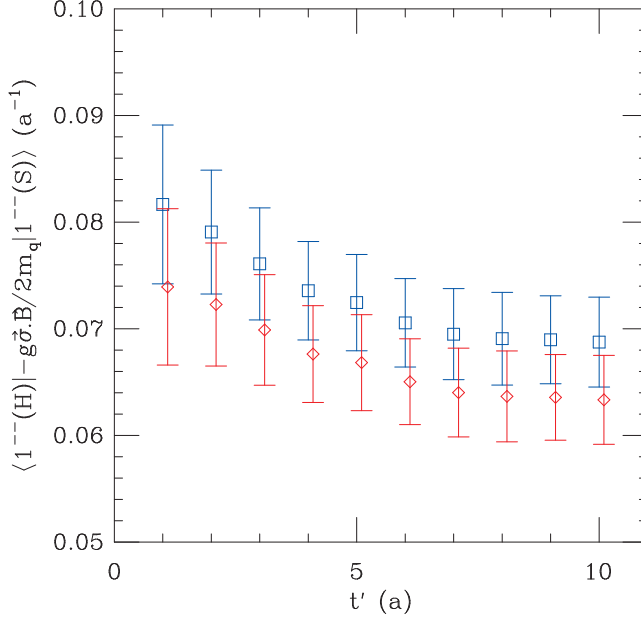


FIG. 3. Magnitude of the off-diagonal matrix element of the Hamiltonian (in lattice units) for the 1^{--} S-wave (source) / hybrid (sink) two-state system vs. the time slice, t' , at which the interaction (δH) is applied. The squares are for $m_q a = 2.5$, the diamonds for $m_q a = 2.8$.

Fits to the “mixed” propagators were also performed and the resulting values for the off-diagonal matrix element of the Hamiltonian appear in Fig. 3, along with the associated jackknife errors. The Hamiltonian was then diagonalized and the admixture of hybrid within the true ground state calculated (see Fig. 4). It may seem odd that the relative errors for $\sin(\theta)$ are much smaller than those for the matrix element. However, the matrix element is quite strongly correlated with the hybrid/S-wave mass difference [$\sin(\theta) \approx \langle H | \vec{\sigma} \cdot \vec{B} | S \rangle / (m_S - m_H)$]. A plateau is reached in these quantities by $t' = 8$. Using the result at $t' = 9$ ($\chi^2/d.o.f. < 1$) and interpolating in the quark mass to $m_b a = 2.6$, we find

$$\begin{aligned} |\Upsilon\rangle &= \cos(\theta) |Q\bar{Q}\rangle + \sin(\theta) |Q\bar{Q}g\rangle \\ &= 0.99826(6) |Q\bar{Q}\rangle - 0.059(1) |Q\bar{Q}g\rangle, \end{aligned} \quad (7)$$

corresponding to 0.0035(1) probability admixture of hybrid in the 1^{--} bottomonium ground state.

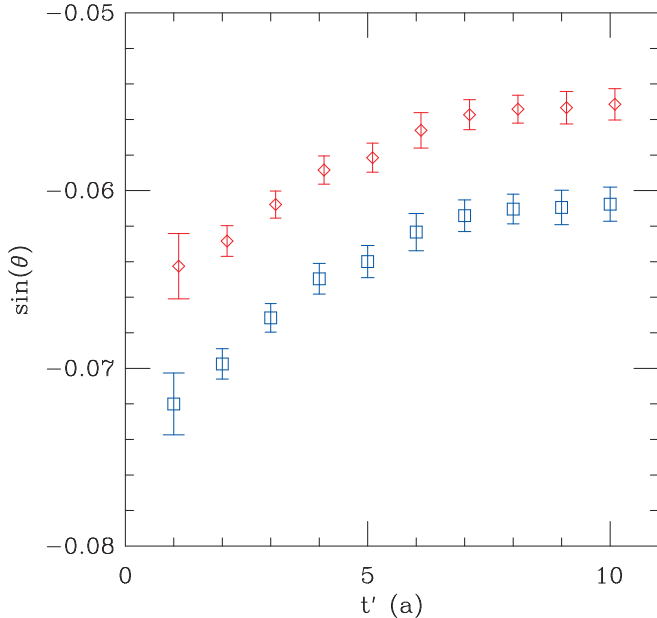


FIG. 4. Mixing angle, $\sin(\theta)$, vs. the time slice, t' , at which the interaction term (δH) is applied. The squares are for $m_q a = 2.5$, the diamonds for $m_q a = 2.8$.

While this result is clearly non-zero, yet low, and therefore consistent with what Drummond *et al.* found, there remain some unresolved issues surrounding the actual number. For one thing, there is the question of the field normalization (i.e., the value for c_B). To get a handle on this number, we performed additional spectrum runs with the interaction “turned on” for all times. The results for these propagator fits can be found in Table III. The resulting $0^{-+}/1^{-}$ mass differences ($\Delta M_{\Upsilon-\eta_b}$) are found to be ~ 20 and ~ 78 MeV for $c_B = 1$ and 2, respectively. While there is currently no experimental result for the η_b mass, there are some potential model calculations [8,9] which predict this splitting to be in the $\sim 30 - 60$ MeV range. This would imply a value of $c_B^2 \sim 1.5 - 3.1$ [$\sin(\theta) \sim 0.073 - 0.104$]. While it is encouraging to find a value of $c_B \sim O(1)$ needed for consistency, a more precise numerical result for this parameter remains elusive, mainly due to the fact that the actual mass splitting is not well known.

It may be noted that our estimate of the hybrid/S-wave mass splitting is quite large, $\Delta M_{1H-1S} = 1.81(12)$ GeV. This is significantly above the 1.644(17) GeV result quoted in Ref. [3] and the recent CP-PACS result of 1.56(18) GeV [10]. However, if we use the lattice spacing as determined by the static quark potential [$a^{-1} = 1.449(4)$ GeV; $m_b a \approx 2.9$], this splitting (which is relatively insensitive to the quark mass) becomes 1.64(12) GeV. It should also be noted, however, that our heavy quark action is simpler (e.g., we leave out the first relativistic correction) than those used by these groups and there is a significant difference in the time resolutions of the lattices used. The CP-PACS result also includes two flavors of light dynamical quarks. It would be useful to resolve these issues with a continuum extrapolation and dynamical lattices as our results thus far are from quenched lattices with only a single value of the coupling.

ACKNOWLEDGEMENTS

This work was supported by the U.S. Department of Energy under contract DE FG03 95ER 40906. Computations were performed on the Nirvana cluster at Los Alamos National Laboratory.

REFERENCES

- [1] W. E. Caswell and G. P. Lepage, Phys. Lett. B **167** (1986) 437; E. Eichten, Nucl. Phys. Proc. Suppl. B **4** (1988) 170; G. P. Lepage and B. A. Thacker, Nucl. Phys. Proc. Suppl. B **4** (1988) 199; G. P. Lepage and B. A. Thacker, Phys. Rev. D **43** (1991) 196.
- [2] T. Manke *et al.*, Phys. Rev. D **57** (1998) 3829; T. Manke *et al.*, Phys. Rev. Lett. **82** (1999) 4396; A. Ali Khan *et al.*, Nucl. Phys. Proc. Suppl. B **83** (2000) 319; K. J. Juge, J. Kuti, and C. J. Morningstar, Nucl. Phys. Proc. Suppl. B **83** (2000) 304.
- [3] I. T. Drummond *et al.*, Phys. Lett. B **478** (2000) 151.
- [4] H. D. Trottier, Phys. Lett. B **320** (1994) 145.
- [5] A. P. Szczepaniak and E. S. Swanson, Phys. Rev. D **55** (1997) 3987.
- [6] G. P. Lepage *et al.*, Phys. Rev. D **46** (1992) 4052.
- [7] C. Bernard *et al.*, Phys. Rev. D **62** (2000) 034503.
- [8] Y.-Q. Chen and R. J. Oakes, Phys. Rev. D **53** (1996) 5051.
- [9] F. J. Yndurain, Nucl. Phys. Proc. Suppl. **93** (2001) 196.
- [10] T. Manke *et al.*, hep-lat/0103015.

TABLES

TABLE I. Meson operators.

J^{PC}	Operator
0^{-+} S-wave (η_b)	$\bar{Q}Q$
1^{--} S-wave (Υ)	$\bar{Q}\sigma_i Q$
0^{++} P-wave (χ_{b0})	$\bar{Q}\sigma_i D_i Q$
1^{++} P-wave (χ_{b1})	$\bar{Q}\varepsilon_{ijk}\sigma_j D_k Q$
2^{++} P-wave (χ_{b2})	$\bar{Q}(\sigma_i D_j + \sigma_j D_i - \frac{2}{3}\delta_{ij}\sigma_k D_k)Q$
0^{-+} hybrid	$\bar{Q}\sigma_i B_i Q$
1^{--} hybrid	$\bar{Q}B_i Q$

TABLE II. Fit results and resulting mass differences (with jackknife errors). For each quantity, the first row is for $m_q a = 2.5$, the second is for $m_q a = 2.8$.

Propagator	Fit range	$m_0 a$	$\chi^2/d.o.f.$
$1^{--}(S)$	9-25	0.4920(2)	13/13
"	9-25	0.4754(2)	16/13
$0^{++}(P)$	5-21	0.767(4)	5.4/13
"	5-21	0.749(4)	5.8/13
$1^{--}(H)$	1-6	1.62(8)	0.16/2
"	1-6	1.62(8)	0.01/2
Quantity		Mass (a^{-1})	Mass (MeV)
ΔM_{1P-1S}	-	0.275(5)	440(fixed)
"	-	0.273(4)	440(fixed)
ΔM_{1H-1S}	-	1.13(8)	1800(120)
"	-	1.14(8)	1840(130)
$M_{1^{--}(S)}^{kinetic}$	-	5.64(6)	9030(100)
"	-	6.36(6)	10230(100)

TABLE III. Fit results and resulting mass differences (with jackknife errors) with the interaction term present at all intermediate time slices. For each quantity, the first row is for $c_B = 1$, the second is for $c_B = 2$ ($m_q a = 2.5$).

Propagator	Fit range	$m_0 a$	$\chi^2/d.o.f.$
$0^{-+}(\text{S})$	8-24	0.4736(2)	20/13
"	8-24	0.4222(2)	14/13
$1^{--}(\text{S})$	8-24	0.4859(2)	12/13
"	8-24	0.4680(3)	7.4/13
$0^{++}(\text{P})$	5-21	0.764(5)	7.8/13
"	5-21	0.737(5)	10/13
$1^{++}(\text{P})$	5-21	0.762(6)	5.8/13
"	5-21	0.737(8)	13/13
$2^{++}(\text{P})$	5-21	0.753(6)	2.1/13
"	5-21	0.721(7)	6.0/13
Quantity		Mass (a^{-1})	Mass (MeV)
$\Delta M_{\chi-\Upsilon}$	-	0.271(5)	440(fixed)
"	-	0.260(7)	440(fixed)
$\Delta M_{\Upsilon-\eta_b}$	-	0.01232(8)	20.0(4)
"	-	0.04583(24)	78(2)